J. Biochem. **139**, 771–777 (2006)
doi:10.1093/jb/mvj090

Convenient Structural Analysis of Glycosphingolipids Using MALDI-QIT-TOF Mass Spectrometry with Increased Laser Power and Cooling Gas Flow

Yusuke Suzuki[1], Minoru Suzuki[1], Emi Ito[1], Naoko Goto-Inoue[1], Kozo Miseki[2], Junko Iida[2], Yuzo Yamazaki[2], Masaki Yamada[2] and Akemi Suzuki[1,*]

[1]*Sphingolipid Expression Laboratory, RIKEN Frontier Research System, Wako, Saitama 351-0198; and* [2]*Shimadzu Corporation, Nakagyo-ku, Kyoto 604-8511*

Received February 6, 2006; accepted February 22, 2006

Matrix-assisted laser desorption/ionization quadrupole ion trap time-of-flight mass spectrometry (MALDI-QIT-TOF MS) was applied to the structural characterization of neutral glycosphingolipids. Lithium adduct ions of glycosphingolipids were analyzed using MALDI-QIT-TOF MS under strong conditions of increased laser power and cooling gas flow. The relative intensities of fragment ions were increased under the strong conditions, and the resulting spectra revealed the presence of oligosaccharide ions fragmented from the glycosphingolipids. Consequently, the oligosaccharide sequences of the glycosphingolipids were readily obtained. To obtain more detailed structural information, MS/MS (MS^2) and MS/MS/MS (MS^3) analyses were performed with selection of the lactosylceramide and ceramide ions, respectively. The resulting data were sufficient to determine the structures of both the oligosaccharide and the ceramide moiety of each glycosphingolipid. The fragmentation patterns of MS^2 and MS^3 for Forssman glycolipid under the strong conditions were comparable to those of MS^3 and MS^4 obtained under standard conditions, respectively. Thus, MALDI-QIT-TOF MS with increased laser power and cooling gas flow is a convenient method for glycosphingolipid analysis.

Key words: alkaline adduct, glycosphingolipids, MALDI-QIT-TOF MS, mass spectrometry.

Abbreviations: CID, collision-induced dissociation; DHB, 2,5-dihydroxybenzoic acid; ESI, electrospray ionization; Gb_3Cer, globotriaosylceramide; Gb_4Cer, globotetraosylceramide; LacCer, lactosylceramide; MALDI, matrix-assisted laser desorption/ionization; MS, mass spectrometry; QIT, quadrupole ion trap; and TOF, time-of-flight.

Glycosphingolipids are a family of membrane components that consist of a hydrophilic carbohydrate chain and a nonpolar ceramide moiety. The ceramide moiety functions to anchor the glycosphingolipid in the membrane (*1–5*). Glycosphingolipids play important roles in a wide variety of cell functions, including cell–cell interactions, cell growth and differentiation, and signaling (*6–10*).

Mass spectrometry (MS) is an indispensable tool for the structural characterization of glycosphingolipids. Soft ionization techniques for MS, such as electrospray ionization (ESI) and matrix-assisted laser desorption/ionization (MALDI) have been applied to glycosphingolipid characterization. Kaga *et al.* characterized lactosylceramide as lithium adducts using MS^n analysis by reverse-phase HPLC-ESI ion-trap MS (*11*). Touboul *et al.* (*12*) characterized glycosphingolipids in urine sediments obtained from patients with Fabry disease using MALDI time-of-flight (TOF) MS, and Hunnam *et al.* (*13*) applied a quadrupole (Q)-TOF mass spectrometer fitted with a MALDI ion source to the analysis of neutral and acidic glycosphingolipids. ESI MS has been used widely to characterize glycosphingolipid mixtures prepared from different biological sources (*14–21*). However, MALDI MS can ionize glycosphingolipids in the presence of contaminating substances, and the introduction of samples into the MS instrument is simpler in MALDI MS than in ESI MS (*22–24*).

Lithium adduct ions are more informative than sodium adduct ions for the structural characterization of ceramides. Therefore, in the present study, lithium adduct ions were generated by adding LiCl to the glycosphingolipid solutions used for MS analysis (*25–30*). A convenient MS method for the structural characterization of lithium adducts of glycosphingolipids was established by employing MALDI-quadrupole ion trap (QIT)-TOF MS, MS/MS (MS^2), and MS/MS/MS (MS^3) with increased laser power and cooling gas flow.

MATERIALS AND METHODS

Materials—Lactosylceramide (LacCer, Galβ1-4Glcβ1-1′Cer), globotriaosylceramide (Gb_3Cer, Galα1-4Galβ-4Glcβ1-1′Cer), and globotetraosylceramide (Gb_4Cer, GalNAcβ1-3Galα1-4Galβ1-4Glcβ1-1′Cer) were purified from human erythrocyte membranes (*31*, *32*). Forssman glycolipid (GalNAcα1-3GalNAcβ1-3Galα1-4Galβ1-4Glcβ1-1′Cer) was purified from sheep erythrocyte membranes (*32*, *33*). NaCl and LiCl were purchased from Sigma-Aldrich Japan (Tokyo, Japan) and Wako Pure Chemical

*To whom correspondence should be addressed. Tel: +81-48-467-9615, Fax: +81-48-462-4692; E-mail: aksuzuki@riken.jp

Industries (Osaka, Japan), respectively. All solvents used for MS were of HPLC grade. Bradykinin and ACTH were obtained from Sigma-Aldrich and used as calibration standards. 2,5-Dihydroxy benzoic acid (DHB) was obtained from Wako Pure Chemical Industries, recrystallized, and used as the matrix.

MALDI-TOF and MALDI-QIT-TOF MS—MALDI-TOF and MALDI-QIT-TOF MS analyses were performed using AXIMA-CFR and AXIMA-QIT mass spectrometers (both from Shimadzu; Kyoto, Japan) in positive ion mode. Ionization was performed with a 337-nm pulsed N_2 laser. The ion-trap chamber was supplied with two separate, independent gases, helium and argon. A continuous flow of helium gas was used for collisional cooling. The pulsed gas, argon, was used to enhance ion cooling and collision-induced fragmentation (*23*). Two ionization conditions were used for MALDI-QIT-TOF MS: the standard conditions employed standard laser power (arbitrary unit 40 of AXIMA-QIT MS) and cooling gas flow, and the strong conditions employed an increased laser power (about twice as powerful as the standard laser) and an increased flow of cooling gas (about 1.5–2 times the standard rate).

The MS spectra were calibrated externally using a standard peptide calibration mixture containing 1 pmol/μl each of bradykinin peptide fragment (amino acid residue 1–7) ($[M+H]^+$, m/z 757.40) and human ACTH peptide fragment (amino acid residue 18–39) ($[M+H]^+$, m/z 2,465.20). A saturated solution of DHB in 40 mM aqueous LiCl was used as the matrix. The glycosphingolipids were prepared as 200 pmol/μl solutions in chloroform:methanol (2:1, v/v). Two microliters each of the matrix and glycolipid solutions were mixed thoroughly, and an aliquot of the resulting mixture was placed on a target plate. The crystallization process was accelerated under a gentle stream of cold air. The target plate carrying co-crystals of matrix and analyte was then introduced into the mass spectrometers.

RESULTS AND DISCUSSION

Structural Characterization of Forssman Glycolipid by MS, MS^2, and MS^3 under the Standard Conditions—The structures of the glycosphingolipids used in this study are shown in Fig. 1. Because lithium adduct ions are more informative than sodium adduct ions for the structural characterization of ceramides (*25–30*), lithium adduct ions were generated by the addition of LiCl to the glycosphingolipid solutions before analysis.

Forssman glycolipid
GalNAcα1-3GalNAcβ1-3Galα1-4Galβ1-4Glcβ1-1'Cer

globotetraosylceramide (Gb_4Cer)
GalNAcβ1-3Galα1-4Galβ1-4Glcβ1-1'Cer

globotriaosylceramide (Gb_3Cer)
Galα1-4Galβ1-4Glcβ1-1'Cer

lactosylceramide (LacCer)
Galβ1-4Glcβ1-1'Cer

Fig. 1. **Structures of the glycosphingolipids used in this study: Forssman glycolipid, globoside or globotetraosylceramide (Gb_4Cer), globotriaosylceramide (Gb_3Cer), and lactosylceramide (LacCer).**

In the MALDI-TOF MS spectrum of Forssman glycolipid, the lithiated molecular ion ($[M+Li]^+$) was detected at m/z 1,548, and no other fragment ions were observed, as shown in Fig. 2. MALDI-QIT-TOF MS^2 with selection of the ion at m/z 1,548 under the standard conditions, as shown in Fig. 3a, resulted in the detection of fragment ions due to the elimination of GalNAc (m/z 1,345), GalNAc-GalNAc (m/z 1,142), GalNAc-GalNAc-Gal (m/z 980), GalNAc-GalNAc-Gal-Gal (m/z 818), and GalNAc-GalNAc-Gal-Gal-Glc (m/z 656). The [GalNAc-GalNAc-Gal + Li] (m/z 575) and [GalNAc-GalNAc + Li] (m/z 413) ions were also detected.

MS^3 of the LacCer ion (m/z 980), the most abundant ion detected by MS^2, was performed for fine structural characterization of the ceramides. In the MS^3 spectrum, the ions resulting from the elimination of Gal (m/z 818) and Gal-Glc (m/z 656, ceramide ion) were detected, as well as the [ceramide – H_2O – HCHO + Li] (m/z 608), [Gal-Glc + Li] (m/z 331), and d18-sphingenine (m/z 289) ions (Fig. 3b). These results demonstrate that the oligosaccharide sequence, ceramide, and sphingosine base of Forssman glycolipid can be characterized by MS^2 and MS^3 analyses of $[M+Li]^+$. The fatty acid of Forssman glycolipid was estimated as the difference in m/z values of the ceramide and sphingenine ions.

MALDI-QIT-TOF MS and MS^2 Analysis of Forssman Glycolipid under the Strong Conditions—The MALDI-QIT-TOF MS spectrum of Forssman glycolipid obtained under the strong conditions is shown in Fig. 4a. Fragment ions resulting from the elimination of GalNAc (m/z 1,345), GalNAc-GalNAc (m/z 1,142), GalNAc-GalNAc-Gal (m/z 980), and GalNAc-GalNAc-Gal-Gal (m/z 818) from the molecular ion were detected. These fragment ions are comparable to those obtained from MS^2 with selection of $[M+Li]^+$ under the standard conditions (Fig. 3a). The LacCer ion (m/z 980) was the most abundant fragment in the MS spectrum under the strong conditions. MS^2 of LacCer ion resulted in the detection of fragment ions due to the elimination of Gal (m/z 818) and Gal-Glc (m/z 656, ceramide ion). The [ceramide – H_2O – HCHO + Li] (m/z 608), [Gal-Glc + Li] (m/z 331), and d18-sphingenine (m/z 289) ions were also detected, as shown in Fig. 4b.

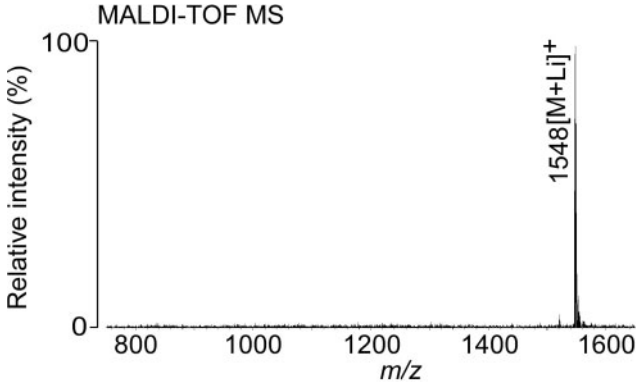

Fig. 2. **MALDI-TOF mass spectrum of Forssman glycolipid after the addition of LiCl.**

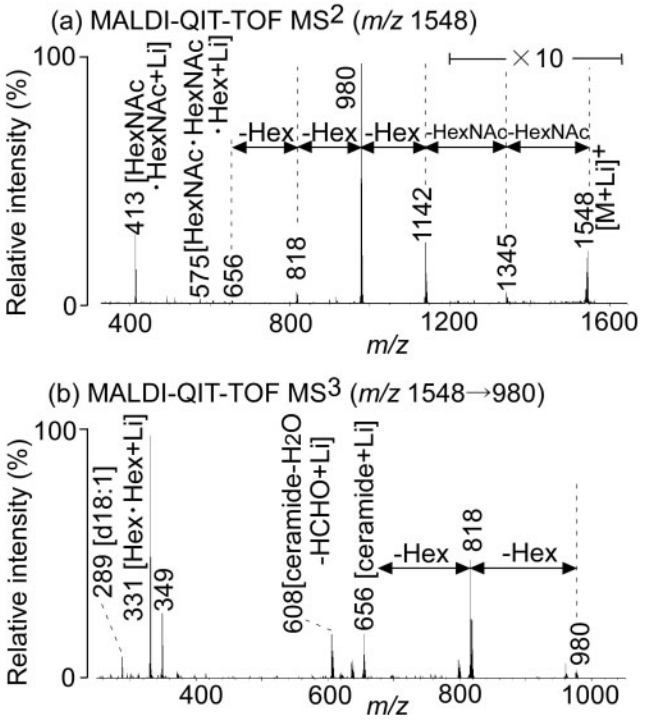

Fig. 3. **MALDI-QIT-TOF MS^2 and MS^3 spectra of Forssman glycolipid obtained under the standard conditions.** (a) MS^2 with selection of the lithiated molecular ion $[M + Li]^+$. (b) MS^3 with selection of the LacCer ion. [d18:1] indicates d18-sphingenine.

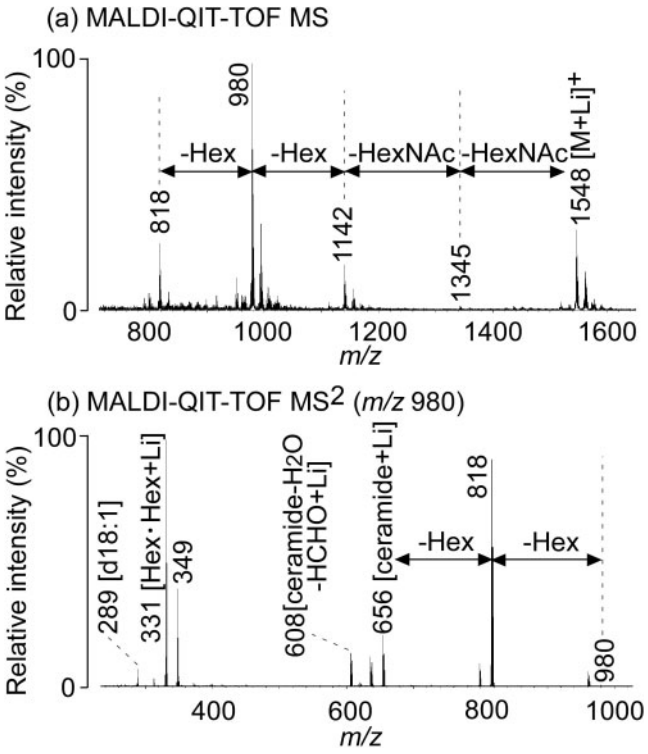

Fig. 4. **MALDI-QIT-TOF MS and MS^2 spectra of Forssman glycolipid obtained under the strong conditions.** (a) MS of Forssman glycolipid. (b) MS^2 with selection of the LacCer ion.

The MS^2 spectrum obtained under the strong conditions contained fragment ions comparable to the MS^3 spectrum obtained by selecting $[M + Li]^+$ under the standard conditions (Figs. 3b and 4b). As a result, MS and MS^2 analyses of the LacCer ion under the strong conditions yielded sufficient information to determine the oligosaccharide sequence of Forssman glycolipid. The fatty acid structure of Forssman glycolipid was estimated as the difference in *m/z* values of the ceramide and sphingenine ions. Both of these values were determined from the MS^2 spectrum obtained under the strong conditions.

MS and MS^2 Analysis of Three Other Glycosphingolipids Using MALDI-QIT-TOF MS under the Strong Conditions— The MALDI-QIT-TOF mass spectrum of Gb_4Cer under the strong conditions is shown in Fig. 5a. Fragment ions resulting from the elimination of GalNAc (*m/z* 1,142), GalNAc-Gal (*m/z* 980), and GalNAc-Gal-Gal (*m/z* 818) from the molecular ion were detected. Furthermore, the MS^2 spectrum of the LacCer ion at *m/z* 980 revealed fragment ions resulting from the elimination of Gal (*m/z* 818) and Gal-Glc (*m/z* 656, ceramide ion), as shown in Fig. 5b. The [ceramide – H_2O – HCHO + Li[(*m/z* 608), [Gal-Glc + Li] (*m/z* 331), and d18-sphingenine (*m/z* 289) ions were also detected. Thus, the oligosaccharide sequence of Gb_4Cer was readily obtained from MS and MS^2 analyses of the LacCer ion. The fatty acid structure of Gb_4Cer was estimated as described in the case of Forssman glycolipid. Both of these values were obtained from the MS^2 spectrum.

The MALDI-QIT-TOF MS spectrum of Gb_3Cer under the strong conditions is shown in Fig. 6a. Fragment ions resulting from the elimination of Gal (*m/z* 980) and Gal-Gal (*m/z* 818) were detected. MS^2 analysis of the LacCer

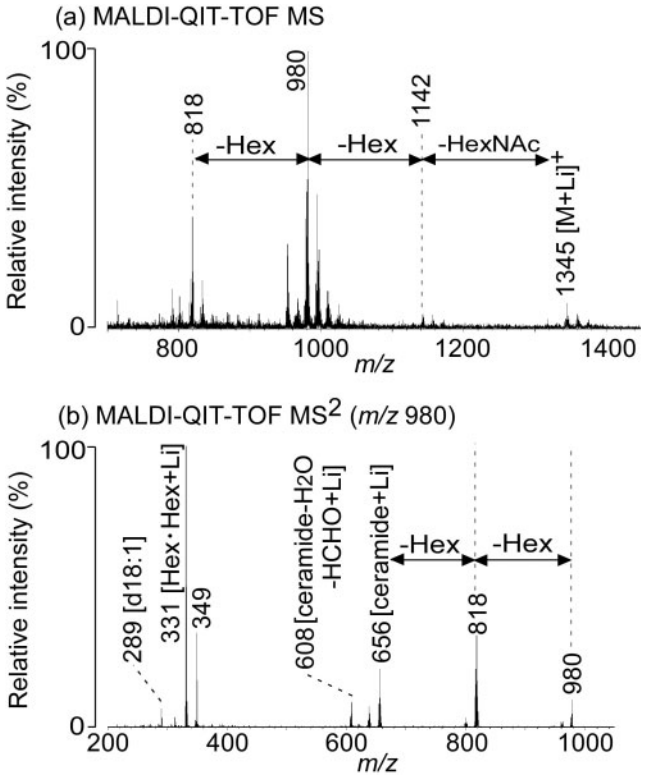

Fig. 5. **MALDI-QIT-TOF MS and MS^2 spectra of Gb_4Cer obtained under the strong conditions.** (a) MS of Gb_4Cer. (b) MS^2 with selection of the LacCer ion.

ion at m/z 980 provided fragment ions resulting from the elimination of Gal (m/z 818) and Gal-Glc (m/z 656, ceramide ion). The [ceramide – H_2O – HCHO + Li] (m/z 608), [Gal-Glc + Li] (m/z 331), and d18-sphingenine (m/z 289) ions were also detected, as shown in Fig. 6b. Thus, MS and MS^2 analyses of the LacCer ion yielded the oligosaccharide sequence of Gb_3Cer. The fatty acid structure of Gb_3Cer was estimated as described above. Both of these values were determined by MS^2 under the strong conditions.

The MALDI-QIT-TOF MS spectrum of LacCer under the strong conditions is shown in Fig. 7a. The LacCer ion was detected as the major peak. The MS^2 spectrum of the LacCer ion at m/z 868 yielded fragment ions resulting from elimination of Gal (m/z 706) and Gal-Glc (m/z 544, ceramide ion). The [ceramide – H_2O – HCHO + Li] (m/z 496), [Gal-Glc + Li] (m/z 331), and d18-sphingenine (m/z 289) ions were also detected, as shown in Fig. 7b. Thus, the oligosaccharide sequence of LacCer was determined by MS and MS^2 analyses of the LacCer ion. The fatty acid structure of LacCer was estimated as described above. Both of these values were determined by MS^2 under the strong conditions.

These results confirm that MALDI-QIT-TOF MS and MS^2 analyses of glycosphingolipids under strong the conditions provide sufficient information to determine the oligosaccharide sequence of glycosphingolipids. Furthermore, the fatty acid structures can be estimated as the difference in m/z values of the ceramide and sphingenine ions, and these values can be obtained by MS^2 under the strong conditions.

MALDI-QIT-TOF MS^3 and MS^4 Analyses for the Fine Characterization of Glycosphingolipid Fatty Acids—To characterize the fatty acids of glycosphingolipids, MALDI-QIT-TOF MS^4 analysis of Forssman glycolipid was performed under the standard conditions, as shown in Fig. 8a. In the MS^4 spectrum, the fragment ions detected included the ceramide ion (m/z 656), a1 (m/z 638), a1–18 (m/z 620), a2 (m/z 608), c2a (m/z 400), d1a (m/z 374), d2a (m/z 356), d1b+d1b′ (m/z 289), d2b (m/z 271), e3b″ (m/z 264), and e3b (m/z 258). These annotations are based on the results reported by Domon and Costello *et al.* (*21*) and Hsu *et al*. (*26*) (Fig. 9). The MS^4 analysis of Forssman glycolipid with selection of the ceramide ion under the standard conditions yielded fragment ions derived from the ceramide fatty acid.

Under the strong conditions, MALDI-QIT-TOF MS^3 of the ceramide ion (m/z 656) of Forssman glycolipid yielded fragment ions a1(m/z 638), a1–18 (m/z 620), a2 (m/z 608), c2a (m/z 400), d1a (m/z 374), d2a (m/z 356), d1b+d1b′ (m/z 289), e2b+e2b′ (m/z 288), d2b (m/z 271), e3b″ (m/z 264), and e3b (m/z 258) (Fig. 8b). Annotations are shown in Fig. 9. The MS^3 analysis of Forssman glycolipid under the strong conditions with selection of the ceramide ion provided information on the fragment ions derived from the fatty acid. The MS^3 spectrum obtained under the strong

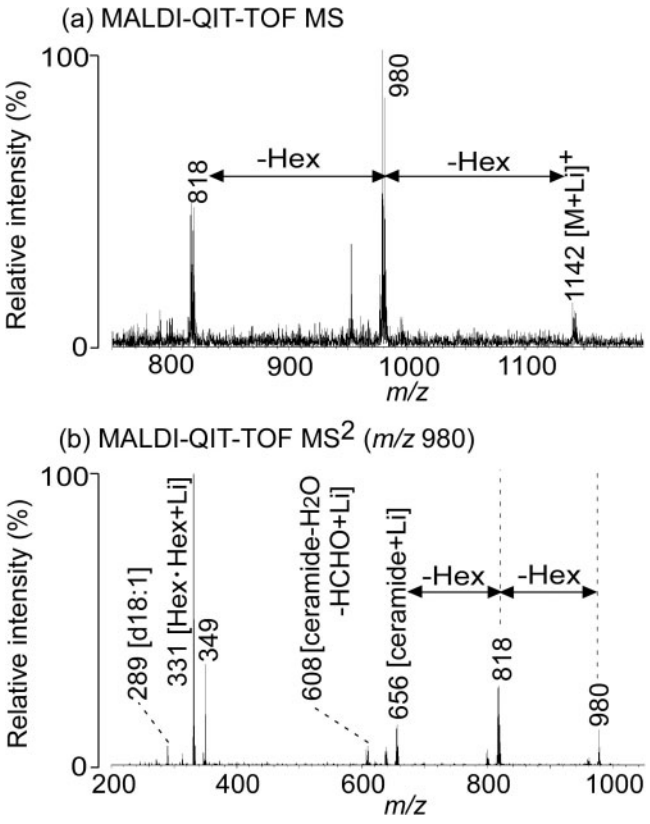

Fig. 6. **MALDI-QIT-TOF MS and MS^2 spectra of Gb_3Cer obtained under the strong conditions.** (a) MS of Gb_3Cer. (b) MS^2 with selection of the LacCer ion.

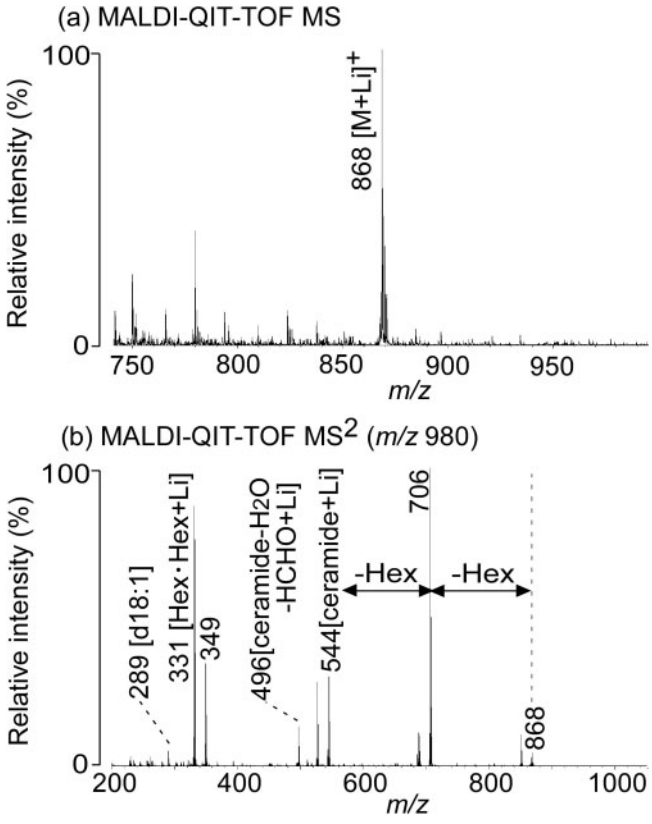

Fig. 7. **MALDI-QIT-TOF MS and MS^2 spectra of LacCer obtained under the strong conditions.** (a) MS of LacCer. (b) MS^2 with selection of the LacCer ion.

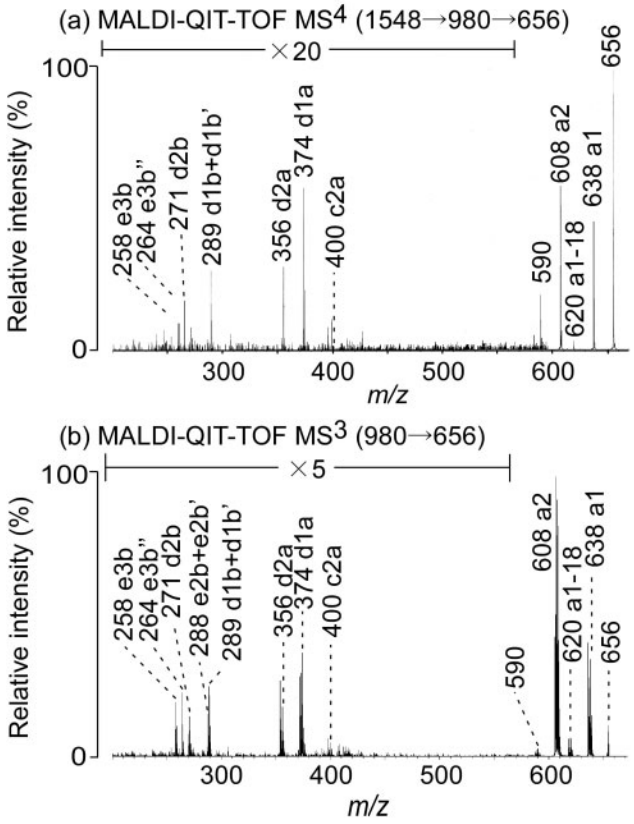

Fig. 8. **MALDI-QIT-TOF MS^3 and MS^4 spectra of Forssman glycolipid with selection of the ceramide ion.** (a) MS^4 spectrum obtained under the standard conditions. (b) MS^3 spectrum obtained under the strong conditions.

conditions is comparable to the MS^4 spectrum obtained by selecting $[M + Li]^+$ under the standard conditions (compare Fig. 8a and b). These results indicate that fatty acid characterization of Forssman glycolipid is achieved by MS^4 analysis under the standard conditions and by MS^3 analysis under the strong conditions.

MALDI-QIT-TOF MS analysis of glycosphingolipids as lithium-adduct ions under the strong conditions provides fragment ions resulting from oligosaccharide elimination, and MS^2 analysis of the LacCer ions yields the oligosaccharide sequence, and ceramide and sphingenine structures. The fatty acid was estimated as the difference in m/z values of the ceramide and sphingenine ions. Furthermore, MS^3 analysis of the ceramide ion under the strong conditions provided fragment ions derived from the fatty acid, and thus the ceramide structure was characterized. In terms of setting the strong conditions, we need to find suitable laser power and cooling gas flow to obtain informative fragmentations. There are adjustment and instrument variations of laser power, and the power is gradually decreased as time passes. Therefore, conditions comparable to the strong conditions in this report have to be found for each MS instrument. In addition, sialic acids of sialylated glycosphingolipids are easily eliminated in MALDI-QIT-TOF MS analysis with the positive ion mode; however, the neutral parts of sialylated glycosphingolipids can be characterized by MALDI-QIT-TOF MS under the strong conditions.

MALDI-QIT-TOF MS analysis of lithium-adduct ions under the conditions of increased laser power and cooling gas flow is a convenient method for the structural characterization of glycosphingolipids. This approach should prove useful for the structural characterization of more complex glycosphingolipids.

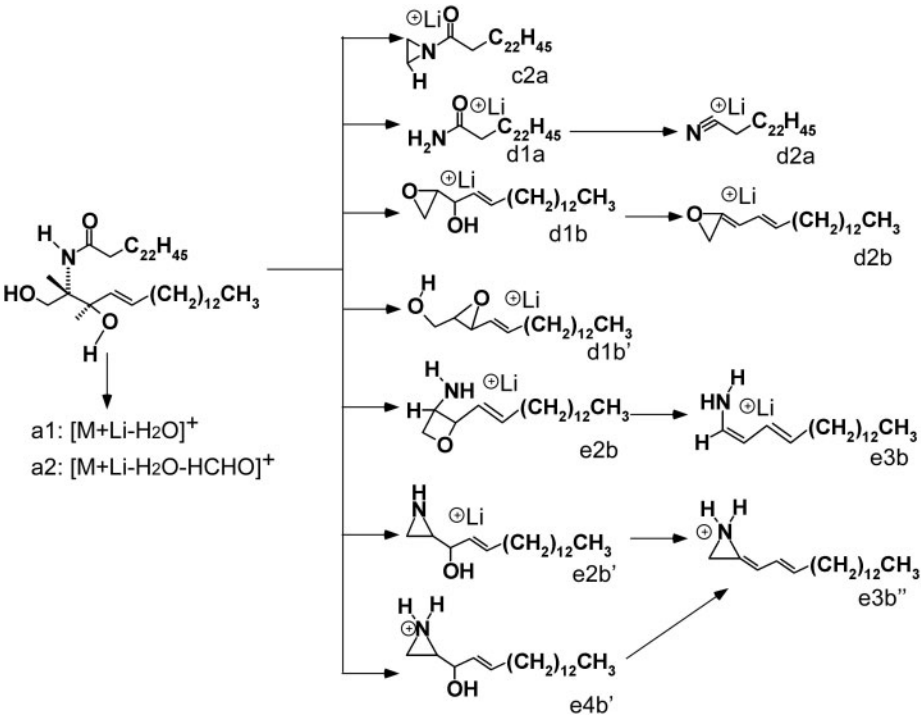

Fig. 9. **Annotation for ceramide fragment ions based on the nomenclature established by Domon and Costello (*21*).** Annotations reported by Hsu *et al.* are cited (*26*).

This work was supported in part by the New Energy and Industrial Technology Development Organization (NEDO) under the Biotechnology Foundation Research Program for Health Maintenance and Improvement in Japan, by the RR project of the Ministry of Education, Culture, Sports, Science, and Technology, by Core Research for Evolutional Science and Technology (CREST), and by the program for the Development of Systems and Technology for Advanced Measurement and Analysis of the Japan Science and Technology Agency (JST).

REFERENCES

1. Karlsson, K.A. (1970) Sphingolipid long chain bases. *Lipids* **5**, 878–891
2. Karlsson, K.A., Samuelsson, B.E., and Steen, G.O. (1973) Detailed structure of sphingomyelins and ceramides from different regions of bovine kidney with special reference to long-chain bases. *Biochim. Biophys. Acta* **316**, 336–362
3. Sastry, P.S. and Kates, M. (1964) Lipid components of leaves. IV. Occurrence of phytosphingosine and dehydrophytosphingosine-containing glucocerebrosides. *Biochim. Biophys. Acta* **84**, 231–233
4. Rosenthal, M.D. (1987) Fatty acid metabolism of isolated mammalian cells. *Prog. Lipid Res.* **26**, 87–124
5. Sandhoff, K. and Kolter, T. (2003) Biosynthesis and degradation of mammalian glycosphingolipids. *Philos. Trans. R. Soc. Lond. B Bio.l Sci.* **358**, 847–861
6. Hakomori, S. (2003) Structure, organization, and function of glycosphingolipids in membrane. *Curr. Opin. Hematol.* **10**, 16–24
7. Hakomori, S., Handa, K., Iwabuchi, K., Yamamura, S., and Prinetti, A. (1998) New insights in glycosphingolipid function: glycosignaling domain, a cell surface assembly of glycosphingolipids with signal transducer molecules involved in cell adhesion coupled with signaling. *Glycobiology* **8**, xi–xix
8. Hakomori, S. and Igarashi, Y. (1995) Functional role of glycosphingolipids in cell recognition and signaling. *J. Biochem.* **118**, 1091–1103
9. Ohanian, J., and Ohanian, V. (2001) Sphingolipids in mammalian cell signalling. *Cell. Mol. Life Sci.* **58**, 2053–2068
10. Hannun, Y.A. and Bell, R.M. (1989) Functions of sphingolipids and sphingolipid breakdown products in cellular regulation. *Science* **243**, 500–507
11. Kaga, N., Kazuno, S., Taka, H., Iwabuchi, K., and Murayama, K. (2005) Isolation and mass spectrometry characterization of molecular species of lactosylceramides using liquid chromatography-electrospray ion trap mass spectrometry. *Anal. Biochem.* **337**, 316–324
12. Touboul, D., Roy, S., Germain, D.P., Baillet, A., Brion, F., Prognon, P., Chaminade, P., and Laprevote, O. (2005) Fast fingerprinting by MALDI-TOF mass spectrometry of urinary sediment glycosphingolipids in Fabry disease. *Anal. Bioanal. Chem.* **382**, 1209–1216
13. Hunnam, V., Harvey, D.J., Priestman, D.A., Bateman, R.H., Bordoli, R.S., and Tyldesley, R. (2001) Ionization and fragmentation of neutral and acidic glycosphingolipids with a Q-TOF mass spectrometer fitted with a MALDI ion source. *J. Am. Soc. Mass Spectrom.* **12**, 1220–1225.
14. Vukelic, Z., Zamfir, A.D., Bindila, L., Froesch, M., Peter-Katalinic, J., Usuki, S., and Yu, R.K. (2005) Screening and sequencing of complex sialylated and sulfated glycosphingolipid mixtures by negative ion electrospray Fourier transform ion cyclotron resonance mass spectrometry. *J. Am. Soc. Mass Spectrom.* **16**, 571–580
15. Merrill, A.H., Jr., Sullards, M.C., Allegood, J.C., Kelly, S., and Wang, E. (2005) Sphingolipidomics: high-throughput, structure-specific, and quantitative analysis of sphingolipids by liquid chromatography tandem mass spectrometry. *Methods* **36**, 207–224
16. McFarland, M.A., Marshall, A.G., Hendrickson, C.L., Nilsson, C.L., Fredman, P., and Mansson, J.E. (2005) Structural characterization of the GM1 ganglioside by infrared multiphoton dissociation, electron capture dissociation, and electron detachment dissociation electrospray ionization FT-ICR MS/MS. *J. Am. Soc. Mass Spectrom.* **16**, 752–762
17. Meisen, I., Peter-Katalinic, J., and Muthing, J. (2004) Direct analysis of silica gel extracts from immunostained glycosphingolipids by nanoelectrospray ionization quadrupole time-of-flight mass spectrometry. *Anal. Chem.***76**, 2248–2255
18. Colsch, B., Afonso, C., Popa, I., Portoukalian, J., Fournier, F., Tabet, J.C., and Baumann, N. (2004) Characterization of the ceramide moieties of sphingoglycolipids from mouse brain by ESI-MS/MS: identification of ceramides containing sphingadienine. *J. Lipid Res.* **45**, 281–286
19. Reinhold, V.N. and Sheeley, D.M. (1998) Detailed characterization of carbohydrate linkage and sequence in an ion trap mass spectrometer: glycosphingolipids. *Anal. Biochem.* **259**, 28–33
20. Domon, B., Vath, J.E., and Costello, C.E. (1990) Analysis of derivatized ceramides and neutral glycosphingolipids by high-performance tandem mass spectrometry. *Anal. Biochem.* **184**, 151–164
21. Domon, B. and Costello, C.E. (1988) Structure elucidation of glycosphingolipids and gangliosides using high-performance tandem mass spectrometry. *Biochemistry* **27**, 1534–1543
22. Shaler, T.A., Wickham, J.N., Sannes, K.A., Wu, K.J., and Becker, C.H. (1996) Effect of impurities on the matrix-assisted laser desorption mass spectra of single-stranded oligodeoxynucleotides. *Anal. Chem.* **68**, 576–579
23. Bajuk, A., Gluch, K., and Michalak, L. (2001) Effect of impurities on the matrix-assisted laser desorption/ionization mass spectra of insulin. *Rapid Commun. Mass Spectrom.* **15**, 2383–2386
24. Amini, A., Dormady, S.J., Riggs, L., and Regnier, F.E. (2000) The impact of buffers and surfactants from micellar electrokinetic chromatography on matrix-assisted laser desorption ionization (MALDI) mass spectrometry of peptides. Effect of buffer type and concentration on mass determination by MALDI-time-of-flight mass spectrometry. *J. Chromatogr. A* **894**, 345–355
25. Afonso, C., Riu, A., Xu, Y., Fournier, F., and Tabet, J.C. (2005) Structural characterization of fatty acids cationized with copper by electrospray ionization mass spectrometry under low-energy collision-induced dissociation. *J. Mass Spectrom.* **40**, 342–349
26. Hsu, F.F., Turk, J., Stewart, M.E., and Downing, D.T. (2002) Structural studies on ceramides as lithiated adducts by low energy collisional-activated dissociation tandem mass spectrometry with electrospray ionization. *J. Am. Soc. Mass Spectrom.* **13**, 680–695
27. Hsu, F.F. and Turk, J. (2001) Structural determination of glycosphingolipids as lithiated adducts by electrospray ionization mass spectrometry using low-energy collisional-activated dissociation on a triple stage quadrupole instrument. *J. Am. Soc. Mass Spectrom.* **12**, 61–79
28. Levery, S.B., Toledo, M.S., Doong, R.L., Straus, A.H., and Takahashi, H.K. (2000) Comparative analysis of ceramide structural modification found in fungal cerebrosides by electrospray tandem mass spectrometry with low energy collision-induced dissociation of Li^+ adduct ions. *Rapid Commun. Mass Spectrom.* **14**, 551–563
29. Hsu, F.F. and Turk, J. (1999) Distinction among isomeric unsaturated fatty acids as lithiated adducts by electrospray ionization mass spectrometry using low energy collisionally activated dissociation on a triple stage quadrupole instrument. *J. Am. Soc. Mass Spectrom.* **10**, 600–612

30. Hsu, F.F. and Turk, J. (1999) Structural characterization of triacylglycerols as lithiated adducts by electrospray ionization mass spectrometry using low-energy collisionally activated dissociation on a triple stage quadrupole instrument. *J. Am. Soc. Mass Spectrom.* **10**, 587–599
31. Ando, S. and Yamakawa, T. (1973) Separation of polar glycolipids from human red blood cells with special reference to blood group-A activity. *J. Biochem.* **73**, 387–396
32. Suzuki, M., Yamakawa, T., and Suzuki, A. (1990) High-performance liquid chromatography-mass spectrometry of glycosphingolipids: II. Application to neutral glycolipids and monosialogangliosides. *J. Biochem.* **108**, 92–98
33. Saito, T. and Hakomori, S.I. (1971) Quantitative isolation of total glycosphingolipids from animal cells. *J. Lipid Res.* **12**, 257–259